Environmental Science & Technology

pubs.acs.org/est

Article

First-Time Isotopic Characterization of Seleno-Compounds in Biota: A Pilot Study of Selenium Isotopic Composition in Top Predator Seabirds

Claudia Marchán-Moreno, Pascale Louvat, Maite Bueno, Sylvain Berail, Warren T. Corns, Yves Cherel, Paco Bustamante, David Amouroux, and Zoyne Pedrero*

Cite This: *Environ. Sci. Technol.* 2024, 58, 13434−13443

Read Online

ACCESS | Metrics & More | Article Recommendations | Supporting Information

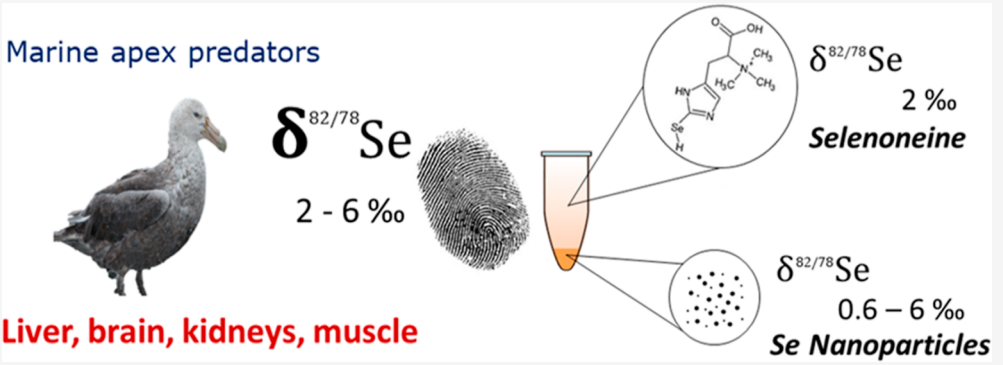

ABSTRACT: This study pioneers the reporting of Se isotopes in marine top predators and represents the most extensive Se isotopic characterization in animals to date. A methodology based on hydride generation—multicollector inductively coupled plasma mass spectrometry—was established for such samples. The study was conducted on various internal organs of giant petrels (*Macronectes* spp.), encompassing bulk tissues ($\delta^{82/78}Se_{bulk}$), distinct Se-specific fractions such as selenoneine ($\delta^{82/78}Se_{SEN}$), and HgSe nanoparticles ($\delta^{82/78}Se_{NPs}$). The $\delta^{82/78}Se_{bulk}$ results (2.0−5.6‰) offer preliminary insights into the fate of Se in key internal organs of seabirds, including the liver, the kidneys, the muscle, and the brain. Notably, the liver of all individuals was enriched in heavier Se isotopes compared to other examined tissues. In nanoparticle fraction, $\delta^{82/78}Se$ varies significantly across individuals ($\delta^{82/78}Se_{NPs}$ from 0.6 to 5.7‰, n = 8), whereas it exhibits remarkable consistency among tissues and individuals for selenoneine ($\delta^{82/78}Se_{SEN}$, 1.7 ± 0.3‰, n = 8). Significantly, there was a positive correlation between the shift from $\delta^{82/78}Se_{bulk}$ to $\delta^{82/78}Se_{SEN}$ and the proportion of Se present as selenoneine in the internal organs. This pilot study proves that Se species-specific isotopic composition is a promising tool for a better understanding of Se species fate, sources, and dynamics in animals.

KEYWORDS: *stable isotopes, selenoneine, HgSe nanoparticles, biota, HG-MC-ICP-MS, giant petrel*

1. INTRODUCTION

Stable selenium (Se) isotopes present mass-dependent fractionation (MDF) and their isotopic shifts are useful indicators of Se fate, sources, and redox reactions in the environment.[1] Measurement of Se isotopic fractionation has been mainly performed in geochemical samples, such as sediments and soils.[1−4] Reports of Se isotopic composition in biological samples are scarce, limited to a few samples of bacteria, yeast, algae, plants, and freshwater fish.[5−8] It is well established that metabolic processes such as uptake, organ biodistribution, and excretion can result in MDF.[9] The study of Se stable isotopes and Se-compound dynamics in living organisms could provide valuable insights on the sources, fate, and reactivity of Se, whose metabolism remains incompletely understood.

Selenium bioaccumulates in marine organisms and, in certain cases, biomagnifies through aquatic food webs.[10] Hence, the seabird's long-life span and high trophic position account for the notably high Se content observed in their tissues, which can reach levels of up to 1000 $\mu g\ g^{-1}$ dry weight in the liver of giant petrels.[11−13] Furthermore, due to their wide-ranging foraging behavior, the examination of seabirds' internal tissues and feathers provides information from distant

Received: March 5, 2024
Revised: June 26, 2024
Accepted: June 27, 2024
Published: July 17, 2024

marine areas. Seabirds are therefore efficiently used as spatial and temporal bioindicators of trace elements and their exposure in the marine environment.[14−16]

Selenium speciation in wild birds has been rarely reported. Recent studies in apex predator seabirds, specifically giant petrels, revealed the presence of mercury selenide nanoparticles (HgSe NPs)[12,17] and selenoneine in several organs.[18] HgSe NPs are considered to be a final product of methylmercury (MeHg) demethylation, and they have been identified in the liver, kidney, muscle, and brain tissue.[12] Although the specific function of selenoneine remains unknown, its strong antioxidant capacity, health benefits,[19−21] and potential role in MeHg detoxification[18,22,23] have raised considerable interest in the research of this relevant Se species. Despite the advances in understanding the role of Se species in seabird metabolism, the protective and/or toxic effects, as well as its role in the detoxification of Hg, are not fully understood.

Regardless of Se biological relevance, Se isotopic values of animal samples have been exclusively reported in three freshwater fishes from a Se-contaminated lake.[5] The lack of studies on Se isotopic composition in biological matrices could be attributed to the multiple analytical difficulties associated with measuring accurate and precise Se isotopic ratios. Nowadays, hydride generation (HG) coupled to multicollector inductively coupled plasma mass spectrometry (HG-MC-ICP-MS) is recognized as the technique of choice for Se stable isotope measurements.[1,24] However, multiple isobaric interferences of Se stable isotopes can occur in plasma, such as $^{40}Ar^{40}Ar$ and $^{38}Ar^{40}Ar$, that could hamper the measurement precision. In addition, for complex biological matrices such as animal tissues, nonspectral interferences due to some transition metals (e.g., Cu, Co, Fe, and Ni) or hydride-forming elements (e.g., As, Ge, and Sb) are expected to occur.[25,26] Therefore, the sample preparation and sample introduction methods should be carefully optimized to minimize these drawbacks.

This work presents a pilot study of Se isotope dynamics in both bulk and Se species-specific fractions of key tissues of a model seabird. A methodology based on HG-MC-ICP-MS was developed for precise total Se and Se species-specific isotopic characterization in biological samples of animal origin. Internal tissues of giant petrels (liver, kidneys, muscle, and brain) and two Se-specific fractions (selenoneine and Se NPs) were studied. These preliminary results mark a key milestone in the understanding of the Se biogeochemical cycle and its interaction with Hg in biota.

2. MATERIALS AND METHODS

2.1. Standard and Reagents. Selenium isotopic standards NIST SRM 3149 (LGC standards) containing 10.11 ± 0.02 mg g^{-1} of selenite [Se(IV)], MERCK Se standard (Merck), and standard solutions of selenite and selenate [Se(VI)] from Spectracer were used. All stock standard solutions were prepared at 10 mgSe L^{-1} in 4% (v/v) HNO_3 and stored at 4 °C. Working standard solutions were prepared by dilution in ultrapure water (Milli-Q, 18.2 MΩ cm, Millipore Bedford, MA, USA) daily. Certified reference materials were investigated along with the samples: dogfish liver DOLT-5 (NRC, Canada), trout muscle ERM-CE101 (JRC, European Union), tuna fish muscle BCR-464 (JRC, European Union), lobster hepatopancreas TORT-2 (NRC, Canada), and Se-enriched yeast SELM-1 (NRC, Canada). Trace Metal grade concentrated HNO_3 (Fisher Chemical, Optima, 67% w/w) and analysis grade concentrated HCl (JT Baker Instra, 36.0−38.5% w/w) were used. Reagents for HG including sodium borohydride (>98%, $NaBH_4$) and reagent grade sodium hydroxide (>98%, NaOH) were purchased from Sigma-Aldrich.

2.2. Sampling Set Description. This work studied seabird samples belonging to two sibling species of giant petrels, the northern (*Macronectes halli*) and southern (*Macronectes giganteus*) giant petrels, which are the dominant seabird scavengers of the Southern Ocean. Details on sample collection and preservation methods are provided in the Supporting Information (Text S1, Table S1). Isolation of HgSe NPs,[18] Hg isotopic characterization,[11] and Se speciation have been carried out in this set of samples. All data relevant to this study are compiled in Table S2 (Text S2).

2.3. Sample Preparation. *2.3.1. Extraction of Se Nanoparticles and Selenoneine-Containing Fractions.* Both Se species-specific fraction isolations were carried out as described elsewhere.[11,17,18] Briefly, fresh samples (conserved at −80 °C) [0.1−0.3 g wet weight (ww)] were homogenized and diluted in 3 mL of ultrapure water. Aqueous extraction was performed using ultrasonication (30 s at 21% of 100 W), followed by centrifugation at 14.5 rpm for 20 min. The water-soluble fraction was removed, filtered with a 0.2 μm PTFE filter, and kept at −4 °C for analysis. For nanoparticle isolation, lyophilized samples were defatted with 3 mL of methanol and softly digested with formic acid. The resulting extract was filtrated using 50 kDa cutoff PTFE filters (Amicon Ultra) and abundantly washed with ultrapure water until total removal of soluble Hg and Se was achieved. Nanoparticles were then recovered by centrifugation for 3 min at 1000*g*.[17]

2.3.2. Total Digestion. All samples, including Se species-specific fractions, were acid digested in the UltraWAVE (Milestone system, Italy) using the procedure outlined by Queipo-Abad et al. (2022).[11] Briefly, all samples (0.01 to 0.5 g) were predigested overnight with concentrated HNO_3 (0.5−5 mL) in a borosilicate-glass tube covered with Teflon caps. The samples were then digested in a single-reaction chamber system. Procedure blanks were also evaluated: concentrated HNO_3 (5 mL) was digested and processed following the same steps as used for the samples. Digestion parameters (temperature of 220 °C and 110 bar pressure) were fixed according to the general method recommended by the manufacturer's application book.[27]

2.3.3. Matrix Prereduction for Isotopic Analysis. For Se isotopic analysis, sample digestion was followed by a prereduction step to guarantee that Se was exclusively present as Se(IV), which is a requirement for HG as Se(VI) does not form a hydride. Digested aliquots (0.5−2 mL) were reduced with 2 mL of concentrated HCl in a closed polypropylene test tube and heated for 2 h at 85 °C in a hot block. The samples were allowed to cool down at room temperature and stored at 4−6 °C for the next preparation step.[6] All Se(IV) standards and prereduced sample solutions were prepared at a concentration of 50 μgSe L^{-1} in 1.7 M HCl for Se isotopic analysis.

2.4. Monitoring of Se Prereduction. Transformation of Se species to Se(IV) after prereduction was monitored by using HPLC-ICP-MS. The HPLC system consisted of an Agilent 1100 series HPLC pump equipped with an autosampler and variable volume sample loop. The analytical column was a Thermo Hypercarb, 5 μm particle size, 100 mm × 4.6 mm I.D. Chromatographic parameters were established according to Dauthieu et al. (2006),[28] and detection conditions are summarized in Table S3. Selenium species in

https://doi.org/10.1021/acs.est.4c02319
Environ. Sci. Technol. 2024, 58, 13434−13443

Table 1. Measurement Accuracy and Reproducibility by the Proposed Methodology Compared to Previous Studies[f]

sample	reference	$\delta^{82/78}$Se	$\delta^{82/77}$Se	$\delta^{82/76}$Se	n
NIST SRM 3149	**this study**	**−0.00 ± 0.26**	**−0.01 ± 0.30**	**0.01 ± 0.35**	**159**
MERCK solution[a]	**this study**[c]	**−0.80 ± 0.21**	**−1.02 ± 0.24**	**−1.26 ± 0.29**	**54**
	this study[d]	**0.92 ± 0.21**	**1.27 ± 0.25**	**1.41 ± 0.33**	**11**
	Far et al.,[6] 2010[29d]	0.99 ± 0.14	1.34 ± 0.16	1.53 ± 0.21	104
	Lanceleur et al., 2015[34] (unpublished results)[d]	0.93 ± 0.22			22
	Carignan & Wen, 2007[30d]	1.03 ± 0.20	1.36 ± 0.20	1.54 ± 0.20	16
	Pons et al., 2020[35]	−0.99 ± 0.04			93
	Rouxel et al., 2002[29]	0.01 ± 0.21	0.04 ± 0.32	0.01 ± 0.24	61
	Chang et al., 2017[36e]	−0.69 ± 0.07	−0.87 ± 0.10	−1.05 ± 0.16	24
	Zhu et al., 2008[37e]			−1.01 ± 0.10	5
SELM-1[b]	**this study**	**−0.69 ± 0.06**	**−0.87 ± 0.11**	**−1.24 ± 0.15**	**3**
	Far et al., 2010[6]	−0.66 ± 0.29	−0.79 ± 0.39	−0.97 ± 0.30	9
	Lanceleur et al., 2015[34] (unpublished results)	−0.42 ± 0.17			3
	Karasiński et al., 2020[33]	−0.54 ± 0.02			3

[a]MERCK solutions correspond to different lots of the standard solutions. Equal suffice has been assigned to those corresponding to the same lot. [b]SELM-1 Se-enriched yeast certified reference material. [c]Corresponding to standard solution named MERCK-1. [d]Corresponding to standard solution named MERCK-2. [e]Corresponding to Merck standard solution (Lot: HC44698550). The lot number is included in the table when described in the cited reference. [f]Mean isotope ratios in Se standard solutions and reference materials (average δ values ±2SD).

the reduced extracts (Section 2.3.1) were tracked by retention times matching with Se(IV) and Se(VI) standard solutions. All solutions were prepared at 1 μgSe L^{-1} in the mobile phase. The injection volume was 100 μL, and a mobile phase flow rate of 1 mL min^{-1} was used. The mobile phase consisted of 240 mmol L^{-1} formic acid and 1% (v/v) methanol, adjusted to pH 2.5 with ammonia.

2.5. Quantification of Se and Other Element Concentrations. Selenium and Hg concentrations were determined by ICP-MS (Agilent 7500) and CV-AFS (PS Analytical 10.025), respectively, as detailed elsewhere.[11] Details are provided in the Supporting Information (Text S2, Table S2).

2.6. Se Stable Isotopes Analysis by HG-MC-ICP-MS. Se isotope ratios were measured with a Nu Plasma 1700 MC-ICP-MS from Nu Instruments (Wrexham, UK). A sample introduction was performed by coupling an online commercial continuous flow HG system CETAC HGX-200 (Figure S1). The instrumental parameters (Table S4) and details on the experimental setup are presented in the Supporting Information (Text S3). Daily optimization of gases and optical lens voltages was performed for maximum stability and sensitivity of the signal, as well as the best peak shape and alignment of the Se peaks. The measurements were made for two 4 week periods: April-2022, and September-October 2022. The overall average sensitivity of 27 sessions was 67 V per 1 μg mL^{-1} of ^{78}Se (67 V ppm^{-1}). One session is defined by a reoptimization of the instrument parameters followed by continuous measurements during the day or overnight.

Selenium isotope ratios were measured by sample-standard bracketing with "on peak zero" subtraction described in detail elsewhere.[29,30] The sequence analysis was as follows: washing, blank, standard, washing, blank, sample, etc. The blank and washing solutions were 1.7 M HCl (in ultrapure water), as were the sample/standard solutions. Washing consisted of a prerinse and then a wash from two different vials of 1.7 M HCl to rapidly return the signal to baseline and limit contamination of the blank solution. Blank measurements were subtracted from sample/standard signals for "on peak zero". The large mass dispersion and the numerous collectors available on the Nu1700 HR-MC-ICP-MS (16 Faraday cups and 5 SEMSs) allowed to monitor simultaneously the intensities of a variety of potential interferences of Se isotopes, such as Br, Kr, SeH, or Ge, that were measured together with Se isotopes (Table S4). Application of the interference corrections following Elwaer & Hintelmann (2008)[31] to a batch of biological sample measurements for Se isotope ratio calculation resulted in no significantly different results compared to direct Se ratio determination. Therefore, we made the choice in this study to not apply any interference corrections other than blank subtraction, as interference corrections could also lead to an overcorrection of the measurements and inaccuracy or lower repeatability. However, the intensities of the possible interferences and their variations among standards and samples were carefully checked.

Results are reported in standard delta notation, as per mil deviations of Se isotope ratios relative to the NIST SRM 3149 standard, and calculated according to the eq 1

$$\delta^{82/78}\text{Se (‰)} = \left(\frac{\delta^{82/78}\text{Se}_{\text{sample}}}{\delta^{82/78}\text{Se}_{\text{NIST 3149}}} - 1 \right) \times 1000 \quad (1)$$

where $^{82/78}\text{Se}_{\text{sample}}$ is the measured $^{82/78}$Se ratio of the sample and $^{82/78}\text{Se}_{\text{standard}}$ is the average of the $^{82/78}$Se ratios of the NIST SRM 3149 standard measured before and after each sample. Data reported for $^{82/77}$Se and $^{82/76}$Se ratios were calculated according to analogue equations.

2.7. Validation of the Methodology for Se Isotopic Analysis. Quality control assessment of precise Se isotope ratio measurements was performed by repeated measurements of NIST SRM 3149 (n = 213), and two MERCK standard solutions (MERCK-1 (n = 74) and MERCK-2 (n = 12)). Measurement precision is represented as two times the standard deviation (±2SD) of a minimum of three analytical replicates. The repeated measurements of these standards during the different sessions yielded a long-term external reproducibility of ±0.20‰ ($\delta^{82/78}$Se, 2SD). Selenium isotopic ratios determined in Se standard solutions and a CRM sample were compared with previously reported values.

Considering the lack of CRMs and reported values for Se isotopes in animal-derived biological samples, we assessed the matrix effect using a standard addition (SA) method. This

https://doi.org/10.1021/acs.est.4c02319
Environ. Sci. Technol. 2024, 58, 13434−13443

involved adding a certified Se isotopic solution (NIST SRM 3149) to various animal samples.[32] The spiked samples were: (1) a fish liver (commercial) as a bulk tissue, (2) the water-soluble fraction of a giant petrel liver (where Se is principally found as selenoneine), and (3) a Se NPs extract from a giant petrel liver. Multielemental quantification of the evaluated matrices is presented in Tables S5 and S6 for the complete set of samples. This was carried out in order to monitor a variety of potential interferences that could hamper the formation of $SeH_{2(g)}$.

3. RESULTS AND DISCUSSION

3.1. Evaluation of Se Recovery during Sample Preparation. HG is the preferred method for precise Se isotope ratio measurements in complex matrices,[24] relying on quantitative Se recovery, reduced interference, and Se concentration preservation.[1] Selenium recovery and matrix composition were evaluated during each step of the sample preparation procedure (Figure S2).

Total matrix digestion (step 1 in Figure S2) was validated by using two CRMs of animal origin. This included a dogfish liver (DOLT-5) and trout muscle tissue (ERM-CE101). In addition, a Se-enriched yeast CRM (SELM-1) was also used. The measured concentrations of the CRMs after the first step were within the certified ranges, thus validating the proposed digestion step for a variety of biological matrices (Table S7).

The Se mass balance during the sample preparation (steps 1 and 2 in Figure S2) showed an overall Se recovery higher than 98%, independent of the matrix (Table S8). In all the reduced extracts (step 2 in Figure S2), corresponding to a variety of matrices which differed in Se and other element concentrations (Table S2), an efficient reduction to Se(IV) was achieved (Figure S3). Consequently, the proposed reduction step guaranteed the complete conversion of Se to its reduced form Se(IV) across a diverse array of biological matrices.

3.2. Se Isotopic Composition in Standard Solutions. A first approach to the evaluation of the method performance was carried out using NIST SRM 3149 as a sample. Table 1 shows that for all Se isotope ratios all δ values are close to zero, with a long-term standard deviation of 0.2 to 0.3‰.

Validation of the method was then achieved by analyzing a commercial Se standard solution (MERCK) and a reference material (SELM-1). This approach is commonly used among different research groups due to the lack of reference materials which have been certified for Se isotopic compositions.[6,33] Two batches of standard solution purchased at different times were measured, named MERCK-1 and MERCK-2. MERCK-2 corresponds to a solution for which delta values have been reported from two studies which have utilized two different MC-ICP-MS instruments.[6,30] All delta values obtained in the present study (Table 1) are within the uncertainties of those previously reported.

Measurements of MERCK-1 over a 6 month period allowed the assessment of its long-term reproducibility (Figure S4). The developed methodology yielded to an average 2SD value of 0.2 to 0.3‰ for all three δ values, similar to the average 2SD reported using different instruments equipped with a collision cell.[29,30] The 2SD values for $\delta^{82/76}$Se in our study and those reported in the literature are higher than those for $\delta^{82/77}$Se and $\delta^{82/78}$Se, despite the larger mass difference between these two Se isotopes. This result can be explained by the combined effect of a higher abundance of the isobaric interferent $^{40}Ar^{36}Ar^{+}$ compared to $^{40}Ar^{38}Ar^{+}$ and $^{40}Ar^{36}ArH^{+}$, and a much lower abundance of the isotope ^{76}Se. Previously, similar findings have been reported for both SSB[6] and double spike methodologies,[36] independently of the mass bias correction strategy.

Although the preparation procedure (Figure S2) resulted in complete Se recovery (>98%) and total transformation to Se(IV), Se reduction has been reported to be the major driver of Se isotopic fractionation.[1] Therefore, the potential isotopic fractionation induced by this step was evaluated. The two MERCK Se standard solutions were prepared following the preparation procedure (step 2 in Figure S2). The Se ratios of the resulting solutions were measured before and after sample reduction. The isotopic values (Table S9) showed a small shift (< −0.2‰) with an apparent enrichment in lighter isotopes in the reduced extract, most probably due to MDF during this reaction step. This apparent systematic shift remains low and negligible considering the average long-term precision of our isotopic measurements' method (2SD = 0.2‰).

3.3. Assessment of the Matrix Effect. Measurement of Se isotopic values by HG-MC-ICP-MS is known to be potentially hampered by the presence of nonspectral interferences due to some transition metals (*e.g.*, Cu, Co, Fe, and Ni) or hydride-forming elements (*e.g.*, As, Ge, and Sb),[25,26] commonly found in animal tissues. Due to the lack of reference materials with available Se isotopic data in biological matrices of animal origin, matrix effects were investigated by the SA method. The mentioned approach has been successfully exploited for Mg and Ca isotopic characterization.[38] This aims to analyze the isotopic compositions of a variety of matrices spiked with the certified Se isotopic solution NIST SRM 3149 in different proportions (Section 2.7). Specifically, the samples used were a fish liver (bulk tissue), the water-soluble fraction (containing >95% of Se as selenoneine) and Se NPs extracted from giant petrel liver (Table S5). These samples have relatively low Se contents (lower than 30 μgSe g^{-1}) in comparison with seabird tissues (up to 445 μgSe g^{-1}) and element/Se molar ratios in the same range (Table S6).

NIST SRM 3149 standard additions were plotted for each of the matrices, with sample to NIST 3149 Se molar ratios ranging from 0.1 to 0.8. Linear regression with $R^2 > 0.9$ values was obtained. Calibration curves were used for the calculation of SA δ values in the samples. A theoretical representation is shown in Figure S5.

The comparison of δ values obtained by direct measurement of the matrix samples and those determined using the SA calibration (Table S10) revealed that the differences lie within the methodology's reproducibility (2SD = 0.2‰), indicating that matrix effects affecting the accuracy of the isotopic measurements for these biological samples were not significant. It is interesting to note that the slight divergences of direct δSe measurements from the SA δ values were raised with the increasing presence of potential interferences and element/Se molar ratios in the following order: standard solutions < Se water-soluble fractions < Se NP extracts < bulk liver tissue (Table S5). In the case of both Se species-specific fractions, Se NPs extracts are characterized by a higher abundance of elements such as Br, Fe, and Zn in comparison to Se (Table S6). This difference in matrix complexity could explain the smaller shift between directly measured and standard δSe values that is observed for water-soluble Se fractions compared to Se NP extracts (Table S10).

It is important also to point out the singular characteristics of this set of samples, for which the measurement of Se

https://doi.org/10.1021/acs.est.4c02319
Environ. Sci. Technol. 2024, 58, 13434−13443

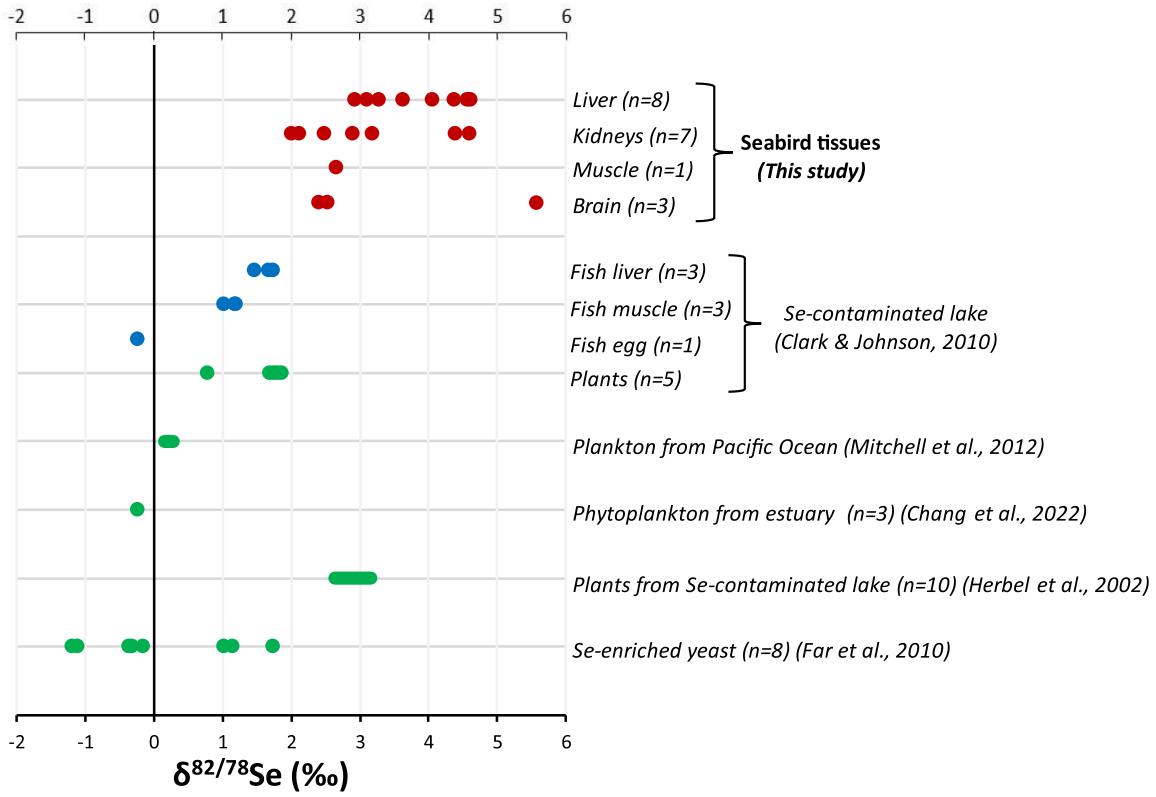

Figure 1. Compilation of published $\delta^{82/78}$Se isotopic ratios for biological samples, including yeast, plants (in green), fish (in blue), and seabird tissues (in red). Selenium values reported by Chang et al. (2022),[40] and Chang et al. (2017)[36] were calculated using the relation: $\delta^{82/78} = 4/6\ \delta^{82/76}$.

isotopic composition was possible using a simple two-step sample preparation. Indeed, the high Se concentration permitted the analysis of largely diluted aliquots of sample, where the interferences/Se molar ratios were minimal (Table S5). To guarantee the precise characterization of Se isotopes in biological samples with lower Se concentrations, further optimization of the sample preparation methodology must be performed, including additional steps to remove the matrix and isolate Se.

3.4. Bulk Se Isotope Distribution in Seabird Tissues. Selenium stable isotopic compositions for a variety of tissues from giant petrels were measured in this study with the validated method summarized in Table S11. The average δSe values obtained were plotted in three-isotope plots,[39] showing linear trends with slopes that matched the theoretical MDF line (95% confidence), as shown in Table S12 and Figure S6. The intercepts found for the experimental MDF lines were close to zero (absolute values <0.036, Table S12) and negligible with respect to the long-term reproducibility of the measurements (2SD = 0.2‰).

Selenium isotope compositions ($\delta^{82/78}Se_{bulk}$) in the seabird tissues vary significantly, ranging from 2.0 to 5.6‰ (Table S11). In contrast to the earlier and limited published results for biological samples, much heavier Se isotopic values were observed in our study (Figure 1). This can be related to the different dietary Se sources and/or to the higher trophic position of seabirds. The measured $\delta^{82/78}Se_{bulk}$ values did not exhibit clear distribution tendencies across organs, possibly attributed to the limited number of individuals/tissues analyzed and the inherent variability among these individuals (*e.g.*, in terms of provenance, age, etc., Tables S1 and S6). However, this work represents, so far, the largest set of Se isotopic ratios in biota. Previous data on Se isotopic composition in biological matrices are predominantly limited to a few samples from Se-contaminated lakes,[5,7,37,40] and commercial Se-enriched yeast (Figure 1).[6] Consequently, interpreting and integrating our results remains challenging due to the limited Se isotopic data in general, especially within biological systems.

In living organisms, Se isotopic fractionation is expected to be induced by metabolic processes affecting Se distribution and molecular fate. Selenium species are involved in multiple-step reactions, and these still need to be fully characterized.

In general, at equilibrium, isotope fractionation is driven by thermodynamic processes, where the phase or site with higher energy bonds (stiff and short bonds) will be preferentially enriched in heavier isotopes.[41] For reactions driven by kinetic processes, isotopic fractionation arises from differences in the vibrational energies of the chemical bonds: those involving lighter isotopes are more easily broken and display a faster reaction rate than those involving heavier isotopes.[1]

The liver consistently exhibits the highest $\delta^{82/78}Se_{bulk}$ value (i.e., heavier Se isotopic composition) within each individual studied (Table S11). This organ acts as a primary target for dietary Se intake, where it is used for various metabolic processes, such as the synthesis of selenoproteins or the production of excretory metabolites.[42] In Se-deficient conditions, it can also distribute Se to other organs.[43] The mechanisms and the extent to which Se is allocated to each of these processes (retention, synthesis, excretion, and redistribution) are not known. However, the enrichment in heavier isotopes in this organ compared to other tissues (Table S11) could be a consequence of the storage of residual Se, which is

https://doi.org/10.1021/acs.est.4c02319
Environ. Sci. Technol. 2024, 58, 13434−13443

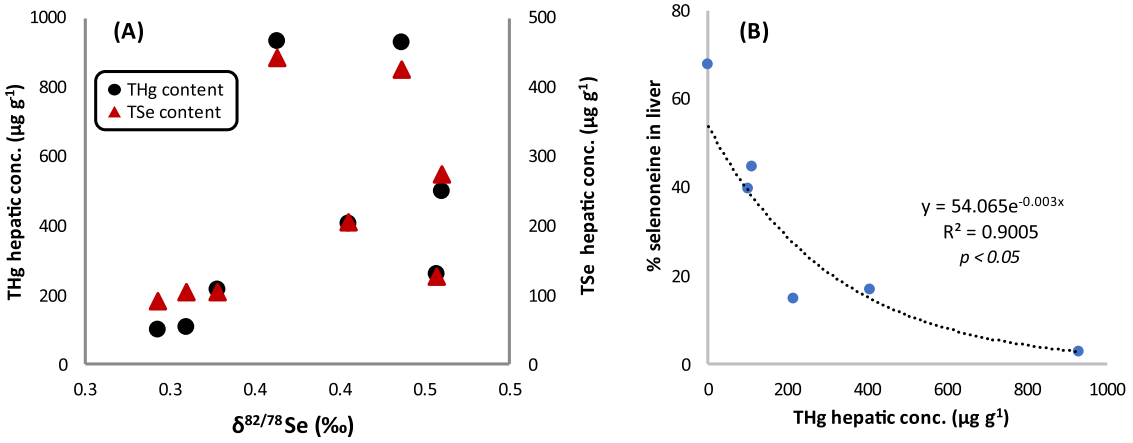

Figure 2. Variation of liver Se isotope ratios (A) and % of selenoneine (B) with the total Se and Hg content. In figure (A), total Hg and Se content are represented by black circles and red triangles, respectively. Figure (B) corresponds to data obtained from El Hanafi et al. (2022).[18]

itself enriched in heavier isotopes, originating from metabolic reactions which are either thermodynamic or kinetic in nature.

Compared to the hepatic Se isotopic signature, a relatively small depletion of $\delta^{82/78}Se_{bulk}$ in the brain (0.56‰, $n = 2$) and muscle (1.7‰, $n = 1$) was observed, while the kidneys exhibited enrichment in lighter isotopes ranging from 1.0 to 2.3‰ ($n = 4$) (Table S11). These results could be understood as a redistribution of Se species from or controlled by the liver pool to other tissues, which consequently are enriched in lighter Se isotopes.

The presence of heavier Se isotopes in the liver compared to other internal organs of giant petrels is in agreement with findings from a prior study conducted on fish:[5] a depletion of heavier isotopes (0.50‰ $\delta^{82/78}Se$) was observed in the fish muscles ($n = 4$) and eggs ($n = 1$) relative to the liver. In the current work, the shift between the Se isotopic signature in muscle and liver seems to be larger (1.7‰ $\delta^{82/78}Se$) (Table S11). Analyses on a larger set of animals would help to better understand such Se isotopic pattern. The enrichment of heavier Hg isotopes in the liver due to their redistribution to other organs has been also described in fish and seabirds.[11,44,45]

Mercury and Se levels in the liver reach values up to 933 $\mu gHg\ g^{-1}$ and 445 $\mu gSe\ g^{-1}$, respectively (Table S2), which are among the highest values ever reported for seabirds.[11] In vertebrates, the liver serves as the primary detoxification and storage organ for Hg, making hepatic concentrations an indirect indicator of an animal's age.[11,46] An increase in hepatic Se concentration with age has been documented in other marine animal species, attributed to the bioaccumulation of this essential element over their lifespan.[47,48] The $\delta^{82/78}Se_{liver}$ values ranged between 2.9 and 4.6‰ (Figure 2). Interestingly, a depletion in heavier Se isotopes (1.1‰) was observed in the livers of animals exhibiting the lowest levels of these elements (Figure 2A). The enrichment in heavier Se isotopes (~5‰) observed in older individuals supports the hypothesis of Se bioaccumulation in the liver across lifetime.[18]

In the liver, Se is primarily associated with the insoluble fraction of the tissue, accounting for more than 55% of the total Se content. The Se/Hg molar ratios in the studied individuals range from 1 to 3 (Table S2), which aligns with the presence of HgSe nanoparticles, constituting over 93% of the total Hg content.[12] The metabolic pathways governing the biomineralization of HgSe nanoparticles are still not fully understood. In this set of samples, selenoneine is the dominant Se species in the water-soluble fraction.[18] The dramatic decrease of selenoneine (from 68 to 3%) with an increase of Hg concentrations in the liver strongly supports the hypothesis of its key role in Hg detoxification.[18] In the current study, we observed Se isotopic signatures with higher $\delta^{82/78}Se$ values in livers with a lower proportion of selenoneine and higher total Hg and Se contents (Figure 2A).

Regarding Se isotopic composition in the brain, there was an enriched heavier isotope ratio on the chick compared to those of older individuals (Figure 3). In this crucial organ,

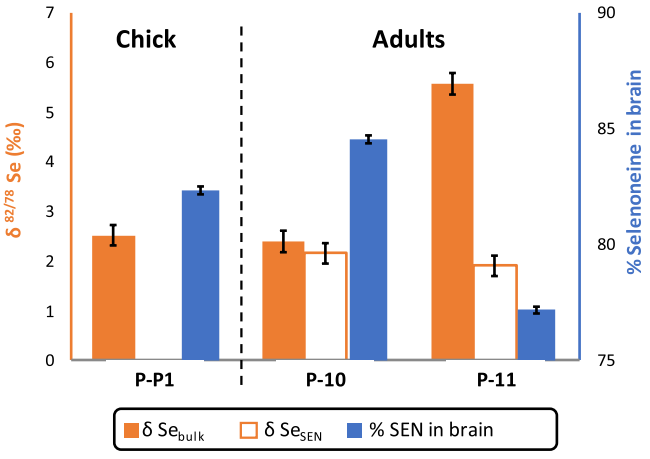

Figure 3. Selenium isotope ratios ($\delta^{82/78}Se$) in bulk (solid color) and water-soluble fractions (clear pattern) of brain tissues are represented in orange bars. Error bars correspond to methodology precision (2SD = 0.2‰). Blue bars correspond to the proportion of selenoneine in brain tissues (data obtained from El Hanafi et al., 2022[18]).

selenoneine represents more than 78% of the total Se content. Interestingly, with age, the fraction of selenoneine increases, while the level of Se associated with other biomolecules remains stable.[18] Considering this singular Se species distribution in relation to age, the 3.1‰ depletion in $\delta^{82/78}Se$ in adults compared to chicks could be attributed to the higher concentrations of selenoneine in the brains of older seabirds, which in turn influences the resulting Se isotopic signature. A more extensive data set involving a larger number of individuals would be required to identify clear trends and selenium pathway dynamics.

https://doi.org/10.1021/acs.est.4c02319
Environ. Sci. Technol. 2024, 58, 13434−13443

3.5. Selenium Species-Specific Isotope Distribution in Seabird Tissues. This study marks the first-ever Se species-specific fraction isotopic characterization (Figure 4). In the current study, we investigated two key seleno-compounds, considering their relevance in biota and their role in Hg detoxification, specifically Se NPs ($\delta^{82/78}$Se NPs) and selenoneine ($\delta^{82/78}Se_{SEN}$) recovered from seabird tissues.

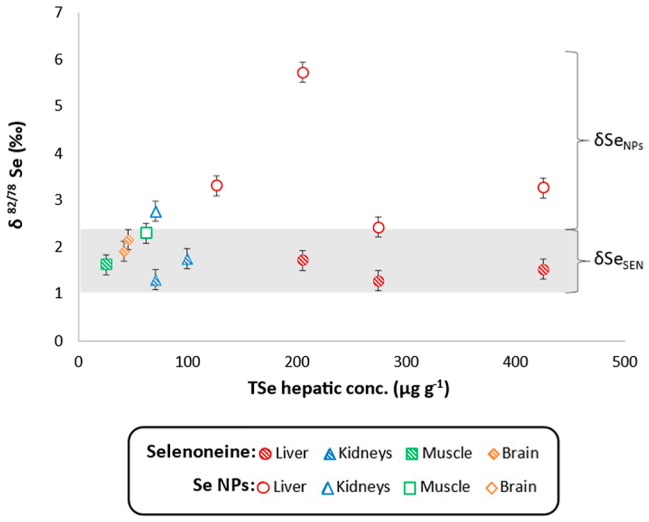

Figure 4. Selenium species isotopic ratios ($\delta^{82/78}Se_{SEN}$ and $\delta^{82/78}Se_{NPS}$) as a function of total Se content in the tissues of seabirds. Error bars correspond to methodology precision (2SD = 0.2‰).

Interestingly, irrespective of tissues or individuals studied, the isotopic signature of selenoneine ($\delta^{82/78}Se_{SEN}$) consistently shows a relatively uniform value (Figure 4), averaging 1.7 ± 0.3‰ (n = 8) (Table S11). Figure 5 illustrates the correlation between the Se fraction present in selenoneine form and the resulting Se isotopic signature in three distinct organs: liver, kidney, and brain.

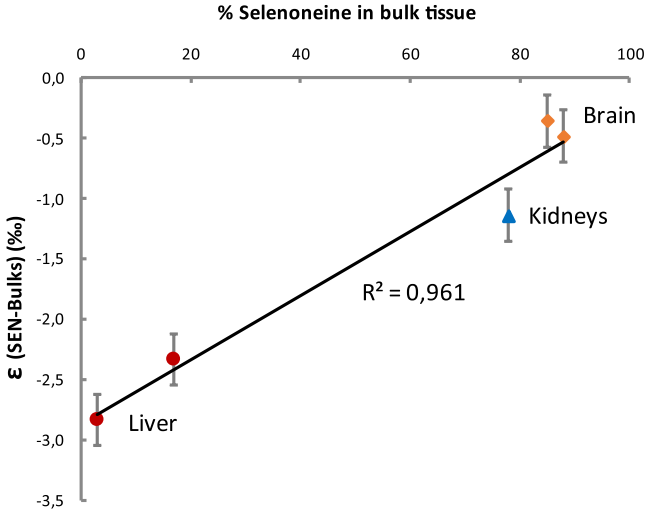

Figure 5. Relation between the selenoneine percent in the tissues and the $\delta^{82/78}$Se shift between water-soluble fraction and bulk tissue, calculated as ε(SEN-bulk) = $\delta^{82/78}Se_{SEN} - \delta^{82/78}Se_{bulk}$. Error bars correspond to methodology precision (2SD = 0.2‰).

The shift in Se isotopic composition between selenoneine fractions and bulk tissues is positively correlated with the proportion of this specific Se species within the internal organs (Figure 5). Liver samples exhibit the highest shift, in absolute terms, between bulk and selenoneine [2.8 ± 0.5‰ (n = 3)], in contrast to the brain, where the isotopic composition in the bulk perfectly matched that of selenoneine (Figure 3).

The described trend not only strongly supports the earlier hypothesis regarding the influence of the Se species-specific $\delta^{82/78}Se_{SEN}$ in δSe of bulk tissues (Section 3.4), but also supports the validation of the methodology employed for the Se-species specific isotopic characterization.

Selenoneine had previously been found in a limited number of biological samples.[18,23,49,50] The sources, biosynthesis, and physiological role of this Se species in biota are still not elucidated.[20−22] This seleno-compound is acknowledged as a potent antioxidant[19,21] and its potential role in HgSe biomineralization has been evoked.[18,23,51] Specific isotopic characterization of Se in this compound could shed light on its reactivity and the mechanisms in which it is involved. Although the data presented here correspond to a limited set of animal samples, they offer preliminary trends in these apex predator seabirds and highlight the necessity of more extensive studies.

Regarding Se NPs extracts, a wide range of $\delta^{82/78}$Se NPs values (Figure 4) from 0.6 to 5.7‰ (n = 8) was observed (Table S11). Despite the limited number of samples in which both Se NPs and selenoneine were simultaneously analyzed, in all organs/individuals, the Se-organic species was depleted by approximately ∼2‰ in comparison to the Se NPs fraction. In the investigated set of samples, any trend was identified regarding the Se isotopic pattern between the bulk and Se NPs.

Similar to how the isotopic composition of Hg in HgSe NPs has recently unveiled new insights into the steps of Hg species biomineralization to HgSe,[11,52] it is expected that characterizing the isotopes of Se within these NPs and along with other Se metabolites, will help elucidate the complex Hg detoxification process. For the moment, this pilot study provides preliminary values, specifically associated with seabirds, and calls for the extension of the isotopic characterization of Se and its species in biota to better understand the fate of Se and its interaction with Hg.

In summary, this work reports for the first time the isotopic composition of Se in Se species-specific fractions in biota. It pioneers the documentation of Se isotopes in seabird tissues and represents the most extensive Se isotopic characterization in animals and organs within biota to date. The Se isotopic signature in the different organs provided preliminary insights on the fate of Se in the key internal organs of seabirds, such as the liver, kidneys, and brain. The specific Se isotopic characterization of relevant seleno-compounds, Se NPs and selenoneine, revealed that while Se in NPs displays great variability between individuals, it remains homogeneous for selenoneine. This pilot isotopic characterization of species-specific fractions of Se in the organs of marine top predators opens new perspectives for the understanding of the fate, sources, and dynamics of Se and its species. Future studies including, individuals of different ages and other Se species, are needed to provide further insights into Se metabolic and biogeochemical pathways in living organisms.

https://doi.org/10.1021/acs.est.4c02319
Environ. Sci. Technol. 2024, 58, 13434−13443

■ ASSOCIATED CONTENT

Supporting Information

The Supporting Information is available free of charge at https://pubs.acs.org/doi/10.1021/acs.est.4c02319.

Additional experimental and results details, including methods conditions and extensive data results (PDF)

■ AUTHOR INFORMATION

Corresponding Author

Zoyne Pedrero − *Universite de Pau et des Pays de l'Adour, E2S UPPA, CNRS, IPREM, Institut des Sciences Analytiques et de Physico-chimie Pour l'Environnement et les Matériaux, Pau 64000, France;* orcid.org/0000-0001-6226-152X; Email: zoyne.pedrerozayas@univ-pau.fr

Authors

Claudia Marchán-Moreno − *Universite de Pau et des Pays de l'Adour, E2S UPPA, CNRS, IPREM, Institut des Sciences Analytiques et de Physico-chimie Pour l'Environnement et les Matériaux, Pau 64000, France;* orcid.org/0000-0002-5916-3328

Pascale Louvat − *Universite de Pau et des Pays de l'Adour, E2S UPPA, CNRS, IPREM, Institut des Sciences Analytiques et de Physico-chimie Pour l'Environnement et les Matériaux, Pau 64000, France*

Maite Bueno − *Universite de Pau et des Pays de l'Adour, E2S UPPA, CNRS, IPREM, Institut des Sciences Analytiques et de Physico-chimie Pour l'Environnement et les Matériaux, Pau 64000, France*

Sylvain Berail − *Universite de Pau et des Pays de l'Adour, E2S UPPA, CNRS, IPREM, Institut des Sciences Analytiques et de Physico-chimie Pour l'Environnement et les Matériaux, Pau 64000, France*

Warren T. Corns − *PS Analytical, Arthur House, Crayfields Industrial Estate, Orpington BR5 3HP, U.K.*

Yves Cherel − *Centre d'Etudes Biologiques de Chizé, UMR 7372 du CNRS—La Rochelle Université, Villiers-en-Bois 79360, France*

Paco Bustamante − *Littoral Environnement et Sociétés (LIENSs), UMR 7266 La Rochelle Université-CNRS, La Rochelle 17000, France;* orcid.org/0000-0003-3877-9390

David Amouroux − *Universite de Pau et des Pays de l'Adour, E2S UPPA, CNRS, IPREM, Institut des Sciences Analytiques et de Physico-chimie Pour l'Environnement et les Matériaux, Pau 64000, France;* orcid.org/0000-0002-0056-8590

Complete contact information is available at: https://pubs.acs.org/10.1021/acs.est.4c02319

Notes

The authors declare no competing financial interest.

■ ACKNOWLEDGMENTS

The authors thank the Agence Nationale de la Recherche (MERSEL Project no. ANR-18-CE34-0004-01) and the Communauté d'Agglomération Pau Béarn Pyrénées (MER-ISOTOP) for their financial support. This project has also received funding from the European Union's Horizon 2020 research and innovation programme under the Marie Skłodowska-Curie grant agreement no. 101007962". C.M.-M. acknowledges their Ph.D. fellowship funded by the Région Nouvelle Aquitaine (Project BENESEL). The authors wish to thank the fieldworkers who collected the samples. Field procedures were authorized by the Ethics Committee of IPEV and by the Comité de l'Environnement Polaire. This study received financial and logistical support from the Institut Polaire Français Paul Emile Victor (IPEV programme no. 109, C. Barbraud) and the Terres Australes et Antarctiques Francaises. P.B. is an honorary member of the IUF (Institut Universitaire de France). The authors would like to acknowledge PS Analytical for their instrumental and technical support.

■ REFERENCES

(1) Johnson, T. M.; Druhan, J. L.; Basu, A.; Jemison, N. E.; Wang, X.; Schilling, K.; Wasserman, N. L. A Review of the Development of Cr, Se, U, Sb, and Te Isotopes as Indicators of Redox Reactions, Contaminant Fate, and Contaminant Transport in Aqueous Systems. *Isotopic Constraints on Earth System Processes*; Wiley, 2022; Vol. *21*, pp 237−269.

(2) Stüeken, E. E. Selenium Isotopes as a Biogeochemical Proxy in Deep Time. *Rev. Mineral. Geochem.* **2017**, *82* (1), 657−682.

(3) Schilling, K.; Johnson, T. M.; Dhillon, K. S.; Mason, P. R. D. Fate of Selenium in Soils at a Seleniferous Site Recorded by High Precision Se Isotope Measurements. *Environ. Sci. Technol.* **2015**, *49* (16), 9690−9698.

(4) Wen, H.; Carignan, J. Selenium Isotopes Trace the Source and Redox Processes in the Black Shale-Hosted Se-Rich Deposits in China. *Geochim. Cosmochim. Acta* **2011**, *75* (6), 1411−1427.

(5) Clark, S. K.; Johnson, T. M. Selenium Stable Isotope Investigation into Selenium Biogeochemical Cycling in a Lacustrine Environment: Sweitzer Lake, Colorado. *J. Environ. Qual.* **2010**, *39* (6), 2200−2210.

(6) Far, J.; Bérail, S.; Preud'homme, H.; Lobinski, R. Determination of the Selenium Isotopic Compositions in Se-Rich Yeast by Hydride Generation-Inductively Coupled Plasma Multicollector Mass Spectrometry. *J. Anal. At. Spectrom.* **2010**, *25* (11), 1695.

(7) Herbel, M. J.; Johnson, T. M.; Tanji, K. K.; Gao, S.; Bullen, T. D. Selenium Stable Isotope Ratios in California Agricultural Drainage Water Management Systems. *J. Environ. Qual.* **2002**, *31* (4), 1146−1156.

(8) Schilling, K.; Johnson, T. M.; Wilcke, W. Isotope Fractionation of Selenium during Fungal Biomethylation by Alternaria Alternata. *Environ. Sci. Technol.* **2011**, *45* (7), 2670−2676.

(9) Tanaka, Y. K.; Hirata, T. Stable Isotope Composition of Metal Elements in Biological Samples as Tracers for Element Metabolism. *Anal. Sci.* **2018**, *34* (6), 645−655.

(10) Stewart, R.; Grosell, M.; Buchwalter, D. B.; Fisher, N. S.; Luoma, S. N.; Mathews, T.; Orr, P.; Wang, W. Bioaccumulation and Trophic Transfer of Selenium. In *Ecological Assessment of Selenium in the Aquatic Environment*; Chapman, P. M., Adams, W. J., Brooks, M. L., Delos, C. G., Luoma, S. N., Maher, W. A., Ohlendorf, H. M., Presser, T. S., Shaw, D. P., Eds.; CRC Press, 2010; pp 93−139.

(11) Queipo-Abad, S.; Pedrero, Z.; Marchán-Moreno, C.; El Hanafi, K.; Bérail, S.; Corns, W. T.; Cherel, Y.; Bustamante, P.; Amouroux, D. New Insights into the Biomineralization of Mercury Selenide Nanoparticles through Stable Isotope Analysis in Giant Petrel Tissues. *J. Hazard. Mater.* **2022**, *425*, 127922.

(12) Manceau, A.; Gaillot, A. C.; Glatzel, P.; Cherel, Y.; Bustamante, P. In Vivo Formation of HgSe Nanoparticles and Hg−Tetraselenolate Complex from Methylmercury in Seabirds—Implications for the Hg−Se Antagonism. *Environ. Sci. Technol.* **2021**, *55* (3), 1515−1526.

(13) Cruz-Flores, M.; Lemaire, J.; Brault-Favrou, M.; Christensen-Dalsgaard, S.; Churlaud, C.; Descamps, S.; Elliott, K.; Erikstad, K. E.; Ezhov, A.; Gavrilo, M.; Grémillet, D.; Guillou, G.; Hatch, S.; Per Huffeldt, N.; Kitaysky, A. S.; Kolbeinsson, Y.; Krasnov, Y.; Langset, M.; Leclaire, S.; Linnebjerg, J. F.; Lorentzen, E.; Mallory, M. L.; Merkel, F. R.; Montevecchi, W.; Mosbech, A.; Patterson, A.; Perret, S.; Provencher, J. F.; Reiertsen, T. K.; Renner, H.; Strøm, H.; Takahashi, A.; Thiebot, J.-B.; Thórarinsson, T. L.; Will, A.;

Bustamante, P.; Fort, J. Spatial Distribution of Selenium-Mercury in Arctic Seabirds. *Environ. Pollut.* **2024**, *343*, 123110.
(14) Carravieri, A.; Bustamante, P.; Labadie, P.; Budzinski, H.; Chastel, O.; Cherel, Y. Trace Elements and Persistent Organic Pollutants in Chicks of 13 Seabird Species from Antarctica to the Subtropics. *Environ. Int.* **2020**, *134*, 105225.
(15) Chastel, O.; Fort, J.; Ackerman, J. T.; Albert, C.; Angelier, F.; Basu, N.; Blévin, P.; Brault-Favrou, M.; Bustnes, J. O.; Bustamante, P.; Danielsen, J.; Descamps, S.; Dietz, R.; Erikstad, K. E.; Eulaers, I.; Ezhov, A.; Fleishman, A. B.; Gabrielsen, G. W.; Gavrilo, M.; Gilchrist, G.; Gilg, O.; Gíslason, S.; Golubova, E.; Goutte, A.; Grémillet, D.; Hallgrimsson, G. T.; Hansen, E. S.; Hanssen, S. A.; Hatch, S.; Huffeldt, N. P.; Jakubas, D.; Jónsson, J. E.; Kitaysky, A. S.; Kolbeinsson, Y.; Krasnov, Y.; Letcher, R. J.; Linnebjerg, J. F.; Mallory, M.; Merkel, F. R.; Moe, B.; Montevecchi, W. J.; Mosbech, A.; Olsen, B.; Orben, R. A.; Provencher, J. F.; Ragnarsdottir, S. B.; Reiertsen, T. K.; Rojek, N.; Romano, M.; Søndergaard, J.; Strøm, H.; Takahashi, A.; Tartu, S.; Thórarinsson, T. L.; Thiebot, J.-B.; Will, A. P.; Wilson, S.; Wojczulanis-Jakubas, K.; Yannic, G. Mercury Contamination and Potential Health Risks to Arctic Seabirds and Shorebirds. *Sci. Total Environ.* **2022**, *844*, 156944.
(16) Furtado, R.; Granadeiro, J. P.; Campioni, L.; Silva, M.; Pereira, E.; Catry, P. Trace Elements' Reference Levels in Blood of Breeding Black-Browed Albatrosses Thalassarche Melanophris from the Falkland Islands. *Environ. Sci. Pollut. Res.* **2020**, *27* (31), 39265−39273.
(17) El Hanafi, K.; Gomez-Gomez, B.; Pedrero, Z.; Bustamante, P.; Cherel, Y.; Amouroux, D.; Madrid, Y. Simple and Rapid Formic Acid Sample Treatment for the Isolation of HgSe Nanoparticles from Animal Tissues. *Anal. Chim. Acta* **2023**, *1250*, 340952.
(18) El Hanafi, K.; Pedrero, Z.; Ouerdane, L.; Marchán-Moreno, C.; Queipo-Abad, S.; Bueno, M.; Pannier, F.; Corns, W. T.; Cherel, Y.; Bustamante, P.; Amouroux, D. First Time Identification of Selenoneine in Seabirds and Its Potential Role in Mercury Detoxification. *Environ. Sci. Technol.* **2022**, *56* (5), 3288−3298.
(19) Yamashita, Y. Discovery of the Strong Antioxidant Selenoneine in Tuna and Selenium Redox Metabolism. *World J. Biol. Chem.* **2010**, *1* (5), 144.
(20) Tohfuku, T.; Ando, H.; Morishita, N.; Yamashita, M.; Kondo, M. Dietary Intake of Selenoneine Enhances Antioxidant Activity in the Muscles of the Amberjack Seriola Dumerili Grown in Aquaculture. *Mar. Biotechnol.* **2021**, *23* (6), 847−853.
(21) Alhasan, R.; Nasim, M. J.; Jacob, C.; Gaucher, C. Selenoneine A Unique Reactive Selenium Species from the Blood of Tuna with Implications for Human Diseases. *Curr. Pharmacol. Rep.* **2019**, *5* (3), 163−173.
(22) Achouba, A.; Dumas, P.; Ouellet, N.; Little, M.; Lemire, M.; Ayotte, P. Selenoneine Is a Major Selenium Species in Beluga Skin and Red Blood Cells of Inuit from Nunavik. *Chemosphere* **2019**, *229*, 549−558.
(23) Little, M.; Achouba, A.; Dumas, P.; Ouellet, N.; Ayotte, P.; Lemire, M. Determinants of Selenoneine Concentration in Red Blood Cells of Inuit from Nunavik (Northern Québec, Canada). *Environ. Int.* **2019**, *127*, 243−252.
(24) Elwaer, N.; Hintelmann, H. Comparative Performance Study of Different Sample Introduction Techniques for Rapid and Precise Selenium Isotope Ratio Determination Using Multi-Collector Inductively Coupled Plasma Mass Spectrometry (MC-ICP/MS). *Anal. Bioanal. Chem.* **2007**, *389* (6), 1889−1899.
(25) Kumar, A. R.; Riyazuddin, P. Chemical Interferences in Hydride-Generation Atomic Spectrometry. *Trends Anal. Chem.* **2010**, *29* (2), 166−176.
(26) Pohl, P. Hydride Generation − Recent Advances in Atomic Emission Spectrometry. *TrAC Trends Anal. Chem.* **2004**, *23* (2), 87−101.
(27) *UltraWAVE-Application Book*; MilestoneSrl; Milestone Srl—Helping Chemists, 2024.
(28) Dauthieu, M.; Bueno, M.; Darrouzes, J.; Gilon, N.; Potin-Gautier, M. Evaluation of Porous Graphitic Carbon Stationary Phase for Simultaneous Preconcentration and Separation of Organic and Inorganic Selenium Species in "Clean" Water Systems. *J. Chromatogr. A* **2006**, *1114* (1), 34−39.
(29) Rouxel, O.; Ludden, J.; Carignan, J.; Marin, L.; Fouquet, Y. Natural Variations of Se Isotopic Composition Determined by Hydride Generation Multiple Collector Inductively Coupled Plasma Mass Spectrometry. *Geochim. Cosmochim. Acta* **2002**, *66* (18), 3191−3199.
(30) Carignan, J.; Wen, H. Scaling NIST SRM 3149 for Se Isotope Analysis and Isotopic Variations of Natural Samples. *Chem. Geol.* **2007**, *242* (3−4), 347−350.
(31) Elwaer, N.; Hintelmann, H. Selective Separation of Selenium (IV) by Thiol Cellulose Powder and Subsequent Selenium Isotope Ratio Determination Using Multicollector Inductively Coupled Plasma Mass Spectrometry. *J. Anal. At. Spectrom.* **2008**, *23* (5), 733.
(32) Bienvenu, J. F.; Provencher, G.; Bélanger, P.; Bérubé, R.; Dumas, P.; Gagné, S.; Gaudreau, E. ·; Fleury, N. Standardized Procedure for the Simultaneous Determination of the Matrix Effect, Recovery, Process Efficiency, and Internal Standard Association. *Anal. Chem.* **2017**, *89* (14), 7560−7568.
(33) Karasiński, J.; Tupys, A.; Yang, L.; Mester, Z.; Halicz, L.; Bulska, E. Novel Approach for the Accurate Determination of Se Isotope Ratio by Multicollector ICP-MS. *Anal. Chem.* **2020**, *92* (24), 16097−16104.
(34) Lanceleur, L.; Tessier, E.; Bueno, M.; Berail, S.; Hakil, F.; Guyoneaud, R.; Amouroux, D. Selenium Volatilization and Isotopic Fractionation Induced by Micro Organisms during Respiratory Reduction of Sulphate and Fumarate. *Prague (Rep. Tchèque), 25th Goldschmidt Conference 2015*, 2015.
(35) Pons, M. L.; Millet, M. A.; Nowell, G. N.; Misra, S.; Williams, H. M. Precise Measurement of Selenium Isotopes by HG-MC-ICPMS Using a 76−78 Double-Spike. *J. Anal. At. Spectrom.* **2020**, *35* (2), 320−330.
(36) Chang, Y.; Zhang, J.; Qu, J.; Xue, Y. Precise Selenium Isotope Measurement in Seawater by Carbon-Containing Hydride Generation-Desolvation-MC-ICP-MS after Thiol Resin Preconcentration. *Chem. Geol.* **2017**, *471*, 65−73.
(37) Zhu, J. M.; Johnson, T. M.; Clark, S. K.; Zhu, X.-K. High Precision Measurement of Selenium Isotopic Composition by Hydride Generation Multiple Collector Inductively Coupled Plasma Mass Spectrometry with a 74Se-77Se Double Spike. *Chin. J. Anal. Chem.* **2008**, *36* (10), 1385−1390.
(38) Tipper, E. T.; Louvat, P.; Capmas, F.; Galy, A.; Gaillardet, J. Accuracy of Stable Mg and Ca Isotope Data Obtained by MC-ICP-MS Using the Standard Addition Method. *Chem. Geol.* **2008**, *257* (1−2), 65−75.
(39) Young, E. D.; Galy, A.; Nagahara, H. Kinetic and Equilibrium Mass-Dependent Isotope Fractionation Laws in Nature and Their Geochemical and Cosmochemical Significance. *Geochim. Cosmochim. Acta* **2002**, *66* (6), 1095−1104.
(40) Chang, Y.; Zhang, J.; Wu, Y.; Jiang, S.; Wang, X. N.; Qu, J. G.; Su, H. Fractionation of Dissolved Selenium Isotopic composition during a Phytoplankton Bloom in an Estuary. *Geochim. Cosmochim. Acta* **2022**, *328*, 153−167.
(41) Blanchard, M.; Balan, E.; Schauble, E. A. Equilibrium Fractionation of Non-Traditional Isotopes: A Molecular Modeling Perspective. *Rev. Mineral. Geochem.* **2017**, *82* (1), 27−63.
(42) Ha, H. Y.; Alfulaij, N.; Berry, M. J.; Seale, L. A. From Selenium Absorption to Selenoprotein Degradation. *Biol. Trace Elem. Res.* **2019**, *192* (1), 26−37.
(43) Burk, R. F.; Hill, K. E. Regulation of Selenium Metabolism and Transport. *Annu. Rev. Nutr.* **2015**, *35* (1), 109−134.
(44) Feng, C.; Pedrero, Z.; Gentès, S.; Barre, J.; Renedo, M.; Tessier, E.; Berail, S.; Maury-Brachet, R.; Mesmer-Dudons, N.; Baudrimont, M.; Legeay, A.; Maurice, L.; Gonzalez, P.; Amouroux, D. Specific Pathways of Dietary Methylmercury and Inorganic Mercury Determined by Mercury Speciation and Isotopic Composition in Zebrafish (Danio Rerio). *Environ. Sci. Technol.* **2015**, *49* (21), 12984−12993.

https://doi.org/10.1021/acs.est.4c02319
Environ. Sci. Technol. 2024, 58, 13434−13443

(45) Renedo, M.; Pedrero, Z.; Amouroux, D.; Cherel, Y.; Bustamante, P. Mercury Isotopes of Key Tissues Document Mercury Metabolic Processes in Seabirds. *Chemosphere* **2021**, *263*, 127777.
(46) Gajdosechova, Z.; Lawan, M. M.; Urgast, D. S.; Raab, A.; Scheckel, K. G.; Lombi, E.; Kopittke, P. M.; Loeschner, K.; Larsen, E. H.; Woods, G.; Brownlow, A.; Read, F. L.; Feldmann, J.; Krupp, E. M. In Vivo Formation of Natural HgSe Nanoparticles in the Liver and Brain of Pilot Whales. *Sci. Rep.* **2016**, *6* (1), 34361.
(47) Bustamante, P.; Morales, C.; Mikkelsen, B.; Dam, M.; Caurant, F. Trace Element Bioaccumulation in Grey Seals Halichoerus Grypus from the Faroe Islands. *Mar. Ecol.: Prog. Ser.* **2004**, *267*, 291−301.
(48) Ogle, R. S.; Maier, K. J.; Kiffney, P.; William, M. J.; Brasher, A.; Melton, L. A.; Knight, A. W. Bioaccumulation of Selenium in Aquatic Ecosystems. *Lake Reservoir Manage.* **1988**, *4* (2), 165−173.
(49) Klein, M.; Ouerdane, L.; Bueno, M.; Pannier, F. Identification in human urine and blood of a novel selenium metabolite, Se-methylselenoneine, a potential biomarker of metabolization in mammals of the naturally occurring selenoneine, by HPLC coupled to electrospray hybrid linear ion trap-orbital ion trap MS. *Metallomics* **2011**, 3 (5), 513−520.
(50) Yamashita, M.; Yamashita, Y.; Ando, T.; Wakamiya, J.; Akiba, S. Identification and Determination of Selenoneine, 2-Selenyl-N α, N α, N α -Trimethyl-l-Histidine, as the Major Organic Selenium in Blood Cells in a Fish-Eating Population on Remote Japanese Islands. *Biol. Trace Elem. Res.* **2013**, *156*, 36−44.
(51) Pedrero Zayas, Z.; Ouerdane, L.; Mounicou, S.; Lobinski, R.; Monperrus, M.; Amouroux, D. Hemoglobin as a Major Binding Protein for Methylmercury in White-Sided Dolphin Liver. *Anal. Bioanal. Chem.* **2014**, *406* (4), 1121−1129.
(52) Bolea-Fernandez, E.; Rua-Ibarz, A.; Vanhaecke, F.; Krupp, E.; Feldmann, J. High-Precision Isotopic Analysis Sheds New Light on Mercury Metabolism in Long-Finned Pilot Whales (Globicephala Melas). *Sci. Rep.* **2019**, *9* (1), 7262.

NOTE ADDED AFTER ASAP PUBLICATION

Due to a production error, this paper was published ASAP on July 17, 2024, with errors in the title. The corrected version was reposted on July 18, 2024.

https://doi.org/10.1021/acs.est.4c02319
Environ. Sci. Technol. 2024, 58, 13434−13443